J Mol Model (2011) 17:235–242
DOI 10.1007/s00894-010-0717-5

ORIGINAL PAPER

Density functional theory study on $(LiNH_2)_n$ (n=1–5) clusters

Su-Qin Zhou · Su-Min Zhou · Tao Hu · Xue-Hai Ju

Received: 10 December 2009 / Accepted: 8 April 2010 / Published online: 29 April 2010

Abstract Geometrical structures and relative stabilities of $(LiNH_2)_n$ (n=1–5) clusters were studied using density functional theory (DFT) at the B3LYP/6-31G* and B3LYP/6-31++G* levels. The electronic structures, vibrational properties, N–H bond dissociation energies (BDE), thermodynamic properties, bond properties and ionization potentials were analyzed for the most stable isomers. The calculated results show that the Li–N and Li–Li bonds can be formed more easily than those of the Li–H or N–H bonds in the clusters, in which NH_2 is bound to the framework of Li atomic clusters with fused rings. The average binding energies for each $LiNH_2$ unit increase gradually from 142 kJ mol^{-1} up to about 180 kJ mol^{-1} with increasing n. Natural bond orbital (NBO) analysis suggests that the bonds between Li and NH_2 are of strong ionicity. Three-center–two-electron Li–N–Li bonding exists in the $(LiNH_2)_2$ dimer. The N–H BDE values indicate that the change in N–H BDE values from the monomer **a1** to the singlet-state clusters is small. The N–H bonds in singlet state clusters are stable, while the N–H bonds in triplet clusters dissociate easily. A study of their thermodynamic properties suggests that monomer **a1** forms clusters (**b1**, **c1**, **d2** and **e1**) easily at low temperature, and clusters with fewer numbers of rings tend to transfer to ones with more rings at low temperature. E_g, E_{HOMO} and E_{av} decrease gradually, and become constant. Ring-like $(LiNH_2)_{3,4}$ clusters possess higher ionization energy (VIE) and E_g, but lower values of E_{HOMO}. Ring-like $(LiNH_2)_{3,4}$ clusters are more stable than other types. A comparison of structures and spectra between clusters and crystal showed that the NH_2 moiety in clusters has a structure and spectral features similar to those of the crystal.

Keywords $(LiNH_2)_n$ (n=1–5) clusters · Density functional theory · Natural bond orbital · Structure and spectrum · Bond dissociation energy · Thermodynamic properties · Hydrogen storage material

Introduction

Since Chen et al. [1] discovered in 2002 that the M–N–H (M is group 1–4 metals and some transition metals) systems might be used as potential new hydrogen storage materials, metal complex hydrides have received considerable attention. Their potential as hydrogen storage materials is due to the high gravimetric density of hydrogen and their light weight. Leng et al. [2] pointed out that $LiNH_2$, $NaNH_2$, $Mg(NH_2)_2$ and $Ca(NH_2)_2$ can play a prominent role in M–N–H hydrogen storage systems, and studied their synthesis and decomposition. To obtain information on the electronic structure and hydrogen storage mechanism of alkali metal and alkaline-earth metal amides, researchers have studied the theoretical geometric structures, bonding properties, charge transitions and vibration spectra of crystal $LiNH_2$ [3, 4], $NaNH_2$ [5] and $Mg(NH_2)_2$ [6, 7]. However, to date there have been no reports concerning $LiNH_2$ clusters. The study

S.-Q. Zhou · S.-M. Zhou · T. Hu
Key Laboratory for Attapulgite Science and Applied Technology of Jiangsu Province,
College of Life Science and Chemical Engineering,
Huaiyin Institution of Technology,
Huaian 223003, People's Republic of China

S.-Q. Zhou · X.-H. Ju (✉)
Institute for Computation in Molecular and Materials Science,
School of Chemical Engineering,
Nanjing University of Science and Technology,
Nanjing 210094, People's Republic of China
e-mail: xhju@mail.njust.edu.cn

of cluster structures and properties plays an important role in the understanding of bonding properties, from the microcosmic to macroscopic fields [8–10]. Because $LiNH_2$ is a new hydrogen storage material of high gravimetric densities of hydrogen, the study of its clusters will be helpful in understanding crystal hydrogen storage mechanisms. Therefore, this paper reports a study of the structures and properties of $(LiNH_2)_n$ (n=1–5) clusters using density functional theory (DFT) at the B3LYP/6-31G* level.

Computational methods

The symmetry of the $LiNH_2$ crystal structure is tetragonal, with space group I_4^- [11, 12]. Based on the $LiNH_2$ crystal structure, we designed a possible model as the initial structure of the clusters. Clusters of $(LiNH_2)_n$ (n=1–5) were optimized using DFT at the B3LYP/6-31G* level [13, 14]. Moreover, electronic structures, vibrational properties, N–H bond dissociation energies, thermodynamic properties, bond properties and ionization potentials were analyzed for the most stable isomers. The binding energies of clusters were calculated from the following equations:

$$\Delta E = E_{DFT}\left[(LiNH_2)_n\right] - n\, E_{DFT}(LiNH_2) \quad (1)$$

$$\Delta ZPE = ZPE\left[(LiNH_2)_n\right] - n\, ZPE(LiNH_2) \quad (2)$$

$$\Delta E_C = \Delta E + \Delta ZPE \quad (3)$$

where $E_{DFT}[(LiNH_2)_n]$ and $ZPE[(LiNH_2)_n]$ are the total energy and zero point energy of $(LiNH_2)_n$ (n=2–5) clusters , respectively; $E_{DFT}(LiNH_2)$ and $ZPE(LiNH_2)$ are the total energy and zero point energy of $LiNH_2$ (n=1), respectively.

For many compounds, bond dissociation energies [BDE_0(A−B)] and enthalpy change [DH_{298}(A−B)] are almost numerically equivalent, and as a consequence the terms ‘bond dissociation energy’ and ‘bond dissociation enthalpy’ often appear interchangeably in the literature [15]. Therefore, at 0 K, the homolytic BDE can be given in terms of Eq. 4 [15]:

$$\begin{aligned} &\text{For} \quad A-B(g) \rightarrow A\bullet + B\bullet \\ &BDE_0(A-B) = E_0(A\bullet) + E_0(B\bullet) - E_0(A-B) \end{aligned} \quad (4)$$

The BDE with ZPE correction is:

$$BDE(A-B)_{ZPE} = BDE_0(A-B) + \Delta ZPE \quad (5)$$

where ΔZPE is the difference between the ZPE of the products and the reactants.

Computations were performed with the Gaussian 03 package [16]. The optimizations were performed without any symmetry restrictions using the default convergence criteria in the programs. All optimized structures were characterized to be true local energy minima on the potential energy surfaces without imaginary frequencies.

Results and discussion

Figure 1 shows all the optimized geometrical structures and symmetry of $(LiNH_2)_n$ (n=1–5) clusters. Table 1 lists the

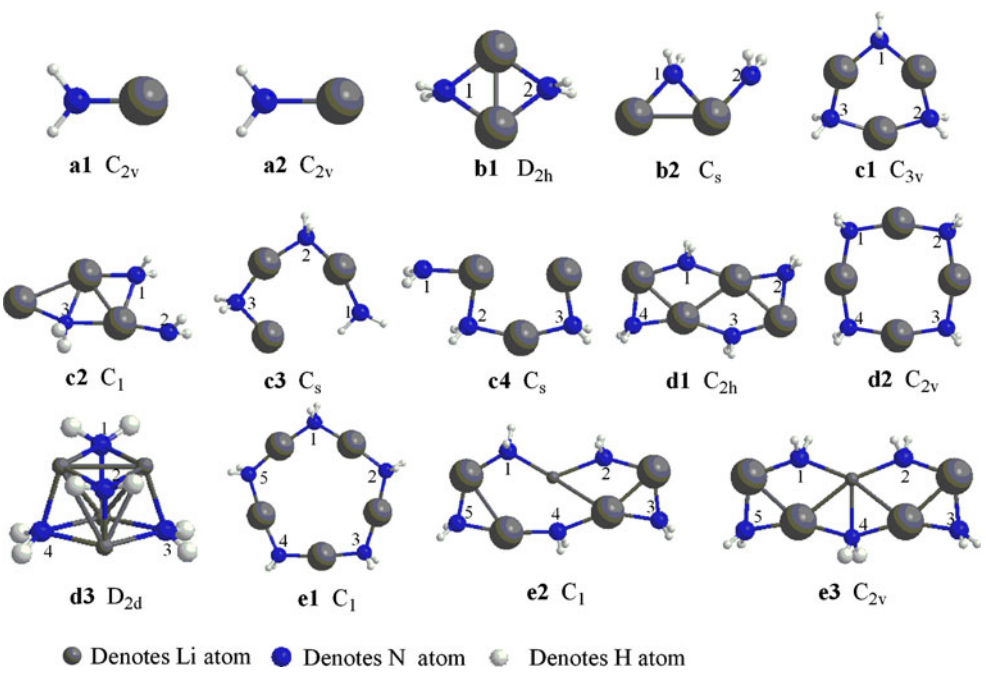

Fig. 1 Geometrical structures and symmetry of $(LiNH_2)_n$ (n=1–5) clusters

Table 1 Geometrical parameters for the most stable structures of $(LiNH_2)_n$ (n=1–5) clusters at the B3LYP/6-31G* level

Cluster	Structure	Bond length/(nm)	Bond angle/(°)
$LiNH_2$	**a1**	Li–N: 0.1740, N–H: 0.1019	Li-N–H: 127.6–127.4, H-N–H: 105.0
$(LiNH_2)_2$	**b1**	Li–N: 0.1913, N–H: 0.1022, Li-Li: 0.2309	N–Li–Li: 53.3, N–Li–N: 106.6, Li–N–Li: 73.4, H–N–H: 103.6, H–N–Li: 119.7
$(LiNH_2)_3$	**c1**	Li–N: 0.1929, N–H: 0.1024	N–Li–N: 143.4–143.6, Li–N–Li: 96.4–96.6, H–N–H: 103.6, H–N–Li: 114.2–114.4
$(LiNH_2)_4$	**d2**	Li–N: 0.1926, N–H: 0.1025	N–Li–N: 161.8, Li–N–Li: 108.2, H–N–H: 103.4, H–N–Li: 111.3–111.4
$(LiNH_2)_5$	**e1**	Li–N: 0.1926, N–H: 0.1025–0.1026	N–Li–N: 172.1–172.8, Li–N–Li: 115.1–115.3, H–N–H: 103.2–103.3, H–N–Li: 109.3–109.7

most stable geometrical parameters at the B3LYP/6-31G* level. Table 2 lists total energies (E_{DFT}), ZPE, uncorrected and corrected binding energies (ΔE and ΔE_c) at the B3LYP/6-31G* and B3LYP/6-31++G* levels.

Optimized geometries and binding energies

As shown in Fig. 1, when n=1, two stably planar structures (**a1** and **a2**) were obtained; their multiplicities are 1 and 3, respectively. They have the same symmetry, but different bond lengths. The **a1** structure has a Li–N distance of 0.1740 nm and two N–H distances of 0.1019 nm, in agreement with the gas-phase structure (Li–N: 0.1736 nm, N–H: 0.1022 nm) measured by millimeter/submillimeter-wave spectroscopy [17]. The **a2** structure has a Li–N distance of 0.2034 nm and two N–H distances of 0.1022 nm. Compared to **a1**, the increment of Li–N distance in **a2** results in its instability as discussed below. Because the triplet state is much more unstable than the singlet state, we therefore concentrated on singlet states for the $(LiNH_2)_2$ clusters. The H–N–H angles of the **a1** and **a2** structures are almost the same, at 105.0° and 105.6°, respectively. When n=2, two stable structures (**b1** and **b2**), one ring-like and the taking a zigzag form, were optimized Their multiplicities are 1 and 3, respectively. When n=3, four stable structures (**c1**–**c4**) were optimized, of which **c1** and **c2** are ring-like and the others chain-like. The multiplicities of **c1** and **c2**–**c4** are 1 and 3, respectively. When n=4, three stable structures (**d1**–**d3**) were obtained, of which **d1** and **d2** are ring-like but **d3** is three-dimensional, with multiplicities of 1. All N–Li–N angles of **d1** are 161.8°. When n=5, three stable structures (**e1**–**e3**) were optimized, all of which are ring-like, but **e2** and **e3** have more rings than **e1**. Their multiplicities are 1. All N–Li–N angles of **e1** are around 172°.

As shown by the optimized structures of $(LiNH_2)_n$ (n= 1–5) clusters, Li–N and Li–Li bonds form more easily than Li–H or N–H bonds in the clusters, and N–N bonds are not

Table 2 Total energies, zero point energy (ZPE) and binding energies of $(LiNH_2)_n$ (n=1–5) clusters[a]. *DFT* Density functional theory

Species	Multiplicity	B3LYP/6-31G*					B3LYP/6-31++G*				
		E_{DFT}	ZPE	ΔE	ΔZPE	ΔE_C	E_{DFT}	ZPE	ΔE	ΔZPE	ΔE_C
a1	1	−63.47148	61.43	0.00	0.00	0.00	−63.48083	61.44	0.00	0.00	0.00
a2	3	−63.38678	57.29	222.39	−4.14	218.26	−63.39019	56.85	237.97	−4.59	233.38
b1	1	−127.05705	137.82	−299.54	14.97	−284.58	−127.06391	136.85	−268.43	13.97	−254.46
b2	3	−126.93349	131.43	24.87	8.57	33.44	−126.94001	131.20	56.87	8.32	65.19
c1	1	−190.62308	208.35	−514.77	24.06	−490.70	−190.63007	206.31	−492.47	21.99	−470.48
c2	3	−190.48966	202.87	−197.47	18.59	−178.88	−190.49895	202.58	−148.21	18.26	−129.95
c3	3	−190.48102	197.39	−174.79	13.10	−161.69	−190.48939	196.01	−123.10	11.69	−111.41
c4	3	−190.48584	201.37	−187.44	17.09	−170.35	−190.49454	200.81	−136.64	16.49	−120.15
d1	1	−254.16651	279.16	−736.67	33.45	−703.22	−254.17659	278.01	−664.93	32.25	−632.68
d2	1	−254.17613	277.88	−761.94	32.17	−729.77	−254.18350	274.74	−683.06	28.98	−654.08
d3	1	−254.16217	279.14	−725.27	33.42	−691.85	−254.17480	278.25	−660.21	32.49	−627.72
e1	1	−317.72296	364.70	−959.58	39.56	−920.19	−317.73160	343.29	−859.69	36.09	−823.60
e2	1	−317.72025	349.01	−952.66	41.87	−910.79	−317.73407	348.48	−866.16	41.28	−824.88
e3	1	−317.72212	349.72	−957.56	42.58	−914.98	−317.73407	348.48	−866.16	41.28	−824.88

[a] E_{DFT} is in Hartree. ZPE, ΔE, ΔZPE and ΔE_C are in kJ mol^{-1}

found in the clusters. All the clusters easily form Li–N fused ring structures, and each N atom links to two H atoms and forms NH_2, which binds to the framework of the Li atom. In addition, H atoms are all stored in the form of NH_2. For the most stable clusters, the bond lengths in $(LiNH_2)_n$ (n=1–5) clusters are 0.1740–0.1929 nm for Li–N and 0.1019–0.1026 nm for N–H bonds , respectively. The N–H bond length coincides with a typical N–H bond length of 0.1010 nm in an NH_3 molecule but is considerably longer than the experimental bond lengths of 0.070 and 0.076 nm found in crystal structure [11]. This discrepancy might be caused by the experimental difficulty in identifying hydrogen positions. The bond angles of H–N–H are 103.2–105.0°, which is consistent with the calculation in crystal (bond length of N–H: 0.1030 nm, bond angle of H–N–H: 102.4°) [12]. As the value of n increases, the bond lengths of Li–N and N–H become longer and approach 0.1926 and 0.1026 nm, respectively; but the bond angle of H–N–H decreases to 103.2°. This shows that the NH_2 moiety in the clusters is consistent with that in crystal.

Furthermore, the atomic arrangement of the **d3** structure is very close to that of the crystal structure. The **d3** configuration has 12 Li–N and 6 Li–Li bonds, of which 8 Li–N bonds lengths are 0.203–0.206 nm, other 4 Li–N bonds lengths are 0.198 nm and 6 Li–Li bonds lengths are 0.23–0.25 nm. These values are in good agreement with those of the crystal [12, 15].

As seen from Table 2, the obtained ΔE_C values at two levels differ slightly, but their change trends are almost identical. Judged by the total binding energies, the most stable isomers are **a1**, **b1**, **c1**, **d2** and **e1**. As n increases, the average binding energies for each $LiNH_2$ unit gradually increase from 142 kJ mol^{-1} in **b1** to 184 kJ mol^{-1} in **e1**, then tend to be constant at around 182 kJ mol^{-1} for **d2** and **e2** at the B3LYP/6-31G* level. In addition, the average binding energies for **e1**, **e2** and **e3** are almost identical at 184, 182 and 183 kJ mol^{-1}, respectively. This shows the average binding energies of clusters are hardly affected by isomers structures for $n \leq 4$.

In addition, the energies of separated products Li + NH_2 relative to the singlet and triplet state of $LiNH_2$ are 254.27 and 36.01 kJ mol^{-1} at the B3LYP/6-31G* level, respectively, and 278.74 and 45.35 kJ mol^{-1} at the B3LYP/6-31++G* level. The energy difference between the singlet and triplet state is 218.26 at the B3LYP/6-31G* level, and 233.39 kJ mol^{-1} at the B3LYP/6-31++G* level, which is consistent with the energy difference between **a2** and **a1**. The triplet states of the $LiNH_2$ dimer and trimer are 320 and 340–359 kJ mol^{-1} above the ground state at the B3LYP/6-31++G* level, respectively.

Vibrational properties

The vibrational frequencies of the most stable isomers for $(LiNH_2)_n$ (n=1–5) clusters were investigated at the B3LYP6-31G* level. Infrared (IR) and Raman spectrums are given in Fig. 2. There are no imaginary frequencies, indicating that the isomers are true minima on the potential energy surface. The calculated results show IR and Raman spectra of $(LiNH_2)_n$ (n=1–5) clusters focus on three regions 45–875, 1,488–1,595 and 3,222–3,452 cm^{-1}. The IR vibrational peaks of all clusters locate in the region 343.49–875.35 cm^{-1}, corresponding mainly to bending vibration of the Li–N–H bond. The 3,222–3,452 cm^{-1} is stretching vibration of N–H bond and the region 1,488–1,595 cm^{-1} is associated with bending of the H–N–H bond. Both regions are characteristic vibration peaks of NH_2. The literature lists symmetrical and asymmetrical N–H stretching vibrations of $Ca(NH_2)_2$, $Mg(NH_2)_2$, $NaNH_2$ and $LiNH_2$, of which the symmetrical N–H stretching vibration lies at 3,228 [18], 3,274 [19] , 3,258 [20] and 3,259 cm^{-1} [21], respectively; while the asymmetrical N–H stretching vibration lies at 3,290 [18], 3,325 [19] and 3,313 cm^{-1} [20, 21], respectively. The literature [22] gave the vibrational frequencies of NH_2, which are 3212.5, 1539.5 and

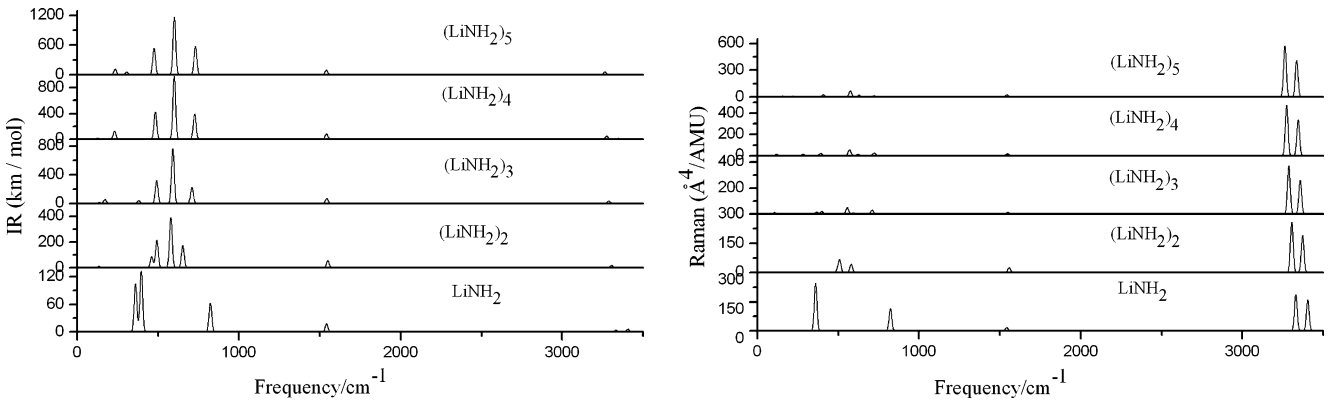

Fig. 2 Vibrational spectra for the most stable configuration of $(LiNH_2)_n$ (n=1–5) clusters

3.0 cm^{-1}. The results calculated herein also include symmetrical and asymmetrical N–H stretching vibrations. After being calibrated by a scaling factor of 0.96, symmetrical and asymmetrical N–H stretching vibrations are 3,266.81–3,335.12 and 3,339.75–3,409.74 cm^{-1}, and the bending vibration of the HN–H bond is 1,538.96–1,559.56 cm^{-1}. These results are consistent with those in crystal, which shows that the structures of NH_2 in clusters and in crystal are identical.

Electron structure

Atomic charges of the most stable singlet isomers for $(LiNH_2)_n$ (n=1–5) clusters were analyzed by the natural bond orbital (NBO) method at the B3LYP/ 6-31G* level. Table 3 presents the atomic charge population for the most stable configuration of $(LiNH_2)_n$ (n=1–5) clusters. As can be seen in Table 3, the Li atomic charges first increase and then decrease, the H atomic charges are more positive, and the N atomic charges are more negative. Upon going from the monomer to clusters, the electronic charges are transferred from H and Li atoms to the N atom, except for the Li atom of **e1**. This charge transfer makes the N atom negatively charged and the Li and H atoms positively charged. The natural charges of Li, N and H atoms are 0.401 to 0.421, −0.942 to−1.024, and 0.267 to 0.312, respectively, which indicates that bonds between Li and NH_2 are of strong ionicity but the N–H bond in the NH_2 moiety is covalent. Because H stored in NH_2 and N–H bonds is of strong covalence, these hydrogen storage materials rarely release H by direct bond rupture, but rather release H by replacing reactions [23, 24].

For the triplet state of $LiNH_2$, the orbitals of the Li and N atoms contribute 86% and 67%, respectively, to the HOMO and HOMO−1 (highest occupied and second highest occupied molecular orbitals, respectively). This implies that one electron of the nitrogen lone pair in the singlet $LiNH_2$ is excited into a higher level of Li vacant orbital, while the other remains on its original lone pair space. Therefore, there is a single nonbonding electron on the N and Li atom in the triplet state of $LiNH_2$. In addition, to explain the Li–N–Li bonding nature of $(LiNH_2)_n$ (n=1–5) clusters, we compared the electronic structure of H_3^+, $(LiCH_2)_2$ and $(LiNH_2)_2$. The total overlap populations among the three centers of H–H–H, Li–C–Li and Li–N–Li are 0.49, 0.53 and 0.41 at the B3LYP/6-31G* level, respectively. Judging by the fact that H_3^+ is 3-center–2-electron, we deduced that the $(LiCH_2)_2$ dimer has strong 3-center–2-electron Li–C–Li bonding, while the $(LiNH_2)_2$ dimer has weak 3-center–2-electron Li–N–Li bonding.

Table 3 Natural bond orbital (NBO) charge in the most stable configuration of $(LiNH_2)_n$ (n=1–5) clusters

Cluster	Structure	NBO charge (e)
$LiNH_2$	**a1**	N:−0.942, Li: 0.409, H: 0.267
$(LiNH_2)_2$	**b1**	N:−0.996, Li: 0.418, H: 0.289
$(LiNH_2)_3$	**c1**	N:−1.021, Li: 0.421, H: 0.300
$(LiNH_2)_4$	**d2**	N:−1.024, Li: 0.412, H: 0.306
$(LiNH_2)_5$	**e1**	N:−1.023 to −1.024, Li: 0.401–0.402, H: 0.310–0.312

N–H bond dissociation energies

Studies of BDE provided useful information for understanding the stability of the title clusters. The stability of the clusters is affected by N–H bond dissociation energies since N–H is weak compared to other types of bonds. Furthermore, N–H dissociation bonds are essential to the release of H_2. Therefore, we present the values of BDE for N–H bonds in a molecule, and discuss and compared the stability of the title clusters. All the N–H bonds for $(LiNH_2)_n$ (n=1–5) clusters were computed at the UB3LYP/6-31G* level. BDE values are listed in Table 4.

The N–H BDE values with ZPE correction are smaller than those of uncorrected BDE_0, but the order of dissociation energies is not affected by ZPE. As can be seen in Table 4, the N–H BDE_{ZPE} values of **a2**, **b2**, **c2**, **c3** and **c4** (their multiplicity is 3) are 61.32–204.44 kJ mol^{-1} while the N–H BDE_{ZPE} values of singlet species are 403.27–424.01 kJ mol^{-1}. From monomer **a1** to the singlet-state clusters, the change in N–H BDE values is small. However, from monomer **a2** to the triplet clusters, the change in N–H BDE values is very large. Furthermore, when the multiplicity of the clusters is 1, the N–H BDE values are only slightly affected by the degree of polymerization of the clusters, structures or N–H bond position. When the multiplicity of the clusters is 3, the N–H BDE values for the same structure are affected by the N–H bond position, and the differences in N–H BDE values are correspondingly larger than those of the singlet clusters.

Judging by the N–H BDE values, we can conclude that the N–H bonds for singlet clusters are stable while the N–H bonds for triplet clusters dissociate easily upon physical stimuli such as heat or mechanic impact.

Thermodynamic properties

On the basis of vibrational analysis and statistical thermodynamics, the thermodynamic functions, entropies (S_T) and thermal correction to enthalpies (H_T^0) obtained by frequency with a scaling factor of 0.96 [25] are listed in Table 5. At temperatures of 200–1,000 K, the values of ΔS_T, ΔH_T and ΔG_T in the processes of **a1** → **b1**, **c1**, **d2** and **e1** are

Table 4 N–H bond dissociation energies (BDE) for $(LiNH_2)_n$ (n = 1–5) clusters at UB3LYP/6-31G* level[a]

Structure	Bond [b]	BDE_0	BDE_{ZPE}	Structure	Bond [b]	BDE_0	BDE_{ZPE}
a1	N–H	456.24	422.64	**d2**	$N_{1,2,3,4}$–H	457.10	422.68
a2	N–H	233.80	204.44	**d3**	$N_{1,2,3,4}$–H	452.97	419.08
b1	$N_{1,2}$–H	456.71	423.30	**e1**	$N_{1,2,3,4,5}$–H	455.85	403.27
b2	$N_{1,2}$–H	132.30	105.29	**e2**	N_1–H	449.15	415.07
c1	$N_{1,2,3}$–H	457.29	423.34		N_2–H	454.65	419.98
c2	$N_{1,2}$–H	107.02	78.53		N_3–H	456.89	423.67
	N_3–H	304.23	272.93		N_4–H	454.90	420.28
c3	$N_{1,2,3}$–H	84.31	61.32		N_5–H	452.40	419.82
c4	$N_{1,3}$–H	96.96	69.99	**e3**	$N_{1,2}$–H	454.04	419.21
	N_2–H	228.35	197.32		N_4–H	456.23	421.93
d1	N_1–H	455.07	420.23		$N_{3,5}$–H	457.30	424.01
	N_2–H	457.12	423.99				

[a] BDE_0 and BDE_{ZPE} are in kJ mol^{-1}

[b] $N_{1,\ldots,n}$–H denotes that the strengths of the N_1–H to N_n–H bonds are identical

Table 5 Thermodynamic properties of the most stable $(LiNH_2)_n$ (n=1–5) clusters (multiplicity=1) at different temperatures[a]

Structure	Temperature K	Cp $Jmol^{-1}K^{-1}$	S_T $Jmol^{-1}K^{-1}$	H_T^0 $kJmol^{-1}$	ΔS_T $Jmol^{-1}K^{-1}$	ΔH_T $kJmol^{-1}$	ΔG_T $kJmol^{-1}$
a1	200	43.33	212.46	7.32			
	298	48.77	230.84	11.85			
	500	55.73	257.85	22.46			
	700	60.27	277.36	34.08			
	800	62.19	285.53	40.21			
	1,000	65.61	299.78	53.00			
b1	200	76.19	265.03	9.72	-159.89	-289.50	-257.52
	298	99.12	300.11	18.42	-161.57	-289.86	-241.71
	500	122.35	357.70	41.11	-158.00	-288.39	-209.39
	700	134.27	400.90	66.86	-153.82	-285.88	-178.21
	800	138.83	419.14	80.52	-151.92	-284.48	-162.94
	1,000	146.55	450.97	109.08	-148.59	-281.50	-132.91
c1	200	122.32	326.96	14.61	-310.42	-498.05	-435.97
	298	156.30	382.71	28.43	-309.81	-497.82	-405.50
	500	191.29	473.04	64.00	-300.51	-494.08	-343.83
	700	209.45	540.51	104.21	-291.58	-488.73	-284.62
	800	216.39	568.94	125.51	-287.65	-485.82	-255.70
	1,000	228.11	618.53	170.00	-280.81	-479.70	-198.89
d2	200	169.37	400.75	20.27	-449.09	-738.78	-648.96
	298	213.61	477.34	39.25	-446.02	-737.92	-605.01
	500	260.15	600.41	87.70	-430.99	-731.91	-516.42
	700	284.59	692.12	142.35	-417.32	-723.74	-431.62
	800	293.93	730.75	171.29	-411.37	-719.32	-390.22
	1,000	309.69	798.09	231.70	-401.03	-710.07	-309.04
e1	200	216.70	489.97	26.30	-572.33	-930.49	-816.02
	298	271.15	587.51	50.45	-566.69	-928.99	-760.12
	500	329.19	743.42	111.83	-545.83	-920.66	-647.75
	700	359.84	859.42	180.95	-527.38	-909.64	-540.47
	800	371.58	908.25	217.54	-519.4	-903.70	-488.18
	1,000	391.35	993.37	293.90	-505.53	-891.29	-385.76

[a] $\Delta S_T = (S_T)_{ii} - n\,(S_T)_i$, $\Delta H_T = (H_T^0 + E_{DFT} + ZPE)_{ii} - n\,(H_T^0 + E_{DFT} + ZPE)_i$, $\Delta G_T = \Delta H_T - T\Delta S_T$, (i=**a1;** ii=**b1**, **c1**, **d2**, **e1**, n=1, 2, 3, 4, 5, respectively)

negative, indicating that these transformations are spontaneously exothermic.

At the same temperature, from monomer (**a1**) to different clusters (**b1**, **c1**, **d2** and **e1**), the values of $-\Delta S_T$,$-\Delta H_T$ and$-\Delta G_T$ increase with increasing *n*. In addition, the values of ΔS_T, ΔH_T and ΔG_T increase from 200 K to 1,000 K for the structures **b1**, **c1**, **d2** and **e1**. Thus, the binding forces of the clusters are weakened as the temperature increases. As can be seen in Table 5, monomer **a1** forms clusters (**b1**, **c1**, **d2** and **e1**) more easily at low temperature, and clusters with large number of rings are produced more easily than those with a small number of rings at low temperature.

Stability

Stability is a physical quality relating to the reaction and electronic properties of a system, such as ionization energy (VIE), gap energy (E_g), average binding energy (E_{av}) and high occupied orbital energy (E_{HOMO}). VIE and E_g of $(LiNH_2)_n$ (n=1–5) clusters were calculated from the following equations:

$$VIE = E_{[(LiNH2)n^+]} - E_{[(LiNH2)n]} \quad (6)$$

$$E_g = E_{HOMO} - E_{LUMO} \quad (7)$$

where $E_{[(LiNH2)n]}^{+}$ is the total energy of $(LiNH_2)_n^+$, $E_{HF}[(LiNH_2)_n]$ is the total energy of $(LiNH_2)_n$, E_{HOMO} is high occupied orbital energy and E_{LUMO} is low unoccupied orbital energy. E_{av} equals the average binding energy divided by the atomic quantity. The calculated E_g value for **a1** is 3.05 eV, which is consistent with calculated $LiNH_2$ crystal results of 3.2 eV [12] and 3.48 eV [26]. The calculated E_g values for **b1**, **c1**, **d1**–**d3** and **e1**–**e3** are around 4.58–5.35 eV, and those of **a2**, **b2** and **c2**–**c3** are around 2.09–2.63 eV. Our calculated E_g values are centered approximately around those from the $LiNH_2$ crystal calculations [12, 26]. Coefficients of E_g values from **b1**, **c1**, **d1**–**d3** and **e1**–**e3** and **a2**, **b2** and **c2**–**c3** to $LiNH_2$ crystal calculating are 1.32–1.67 and 0.6–0.82, respectively. This indicates that $(LiNH_2)_n$ clusters of the triplet state are much more unstable than those of singlet state.

Figure 3 shows the changes in the connection of VIE, E_g, E_{HOMO} and E_{av} with cluster size. VIE, E_g and E_{HOMO} of clusters change with varying cluster size. Ring-like $(LiNH_2)_{3,4}$ clusters possess higher VIE and E_g but lower E_{HOMO}, indicating that they are more dynamically stable than the others. The average binding energy (E_{av}) decreases gradually and becomes constant because inter-atomic bonding becomes saturated and cluster structures are close to crystal structures with the increasing number of atoms.

Furthermore, we investigated the case of $LiNH_2$ losing a hydrogen atom and converting to LiNH at the B3LYP/6-31++G* level. The optimized LiNH is linear, and its electronic state is $^2\Sigma$, whereas the well-known triatomic NH_2 has both linear and a V-shape structures, corresponding to the electronic states of ^{2}A and ^{2}B, respectively, and the ^2A–^2B energy difference is 165.65 kJ mol^{-1}. The calculated electron affinities (EA) of LiNH, NH_2 and NH are 0.27, 0.61 and 0.37 eV, respectively, i.e., the EAs of NH_2 and NH are in good agreement with the experimental values of $EA_{NH2} = 0.779 \pm 0.037$ eV and $EA_{NH} = 0.38 \pm 0.03$ eV [27].

Conclusions

Based on DFT computations for $(LiNH_2)_n$ (n=1–5) clusters, the following conclusions can be drawn:

(1) The clusters easily form Li–N adjoining ring-like structures, in which NH_2 is bound to the framework of Li atomic clusters. Li–N and Li–Li bonds form easily in the clusters. The bond lengths in $(LiNH_2)_n$ (n=1–5) clusters are 0.1740–0.1929 nm for Li–N and 0.1019–0.1026 nm for N–H bonds, respectively. The bond angles of H–N–H are 103.2–105.0°. The atomic

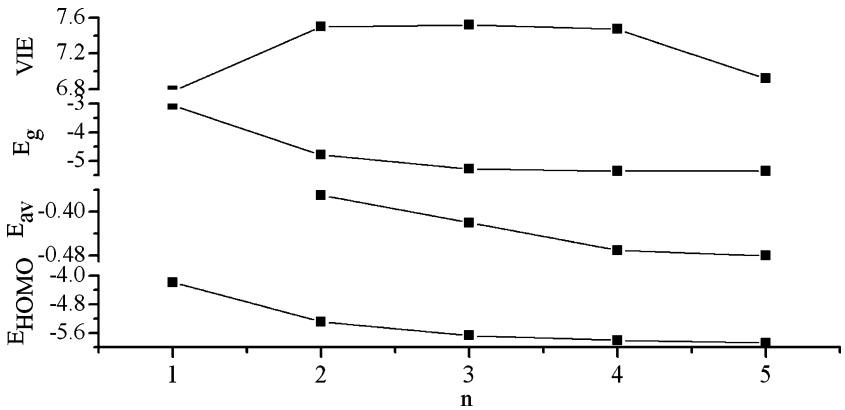

Fig. 3 Ionization energy (VIE), E_g, E_{av} and E_{HOMO} (in eV) of the $(LiNH_2)_n$ (n=1–5) clusters

arrangement of the **d3** structure is very close to that of the crystal structure. The average binding energies for each $LiNH_2$ unit increase gradually to a constant value of about 180 kJ mol^{-1} with increasing n. The energy difference between the singlet and triplet state of $LiNH_2$ is 218.26 at the B3LYP/6-31G* level, and 233.39 kJ mol^{-1} at the B3LYP/6-31++G* level.

(2) IR and Raman spectra of $(LiNH_2)_n$ (n=1–5) clusters focus on three regions of 45–875, 1,488–1,595 and 3,222–3,452 cm^{-1}. Both 1,488–1,595 cm^{-1} and 3,222–3,452 cm^{-1} regions are characteristic vibrational spectra of NH_2. The comparative study of structures and spectra between clusters and crystal shows that the structure of NH_2 in clusters is consistent with that in crystal.

(3) Electronic charge is transferred from H and Li atoms to the N atom on going from the monomer to the clusters, except for **e1**. The bonds between Li and NH_2 are strongly ionic but the N–H bond in the NH_2 moiety is covalent. There is a single nonbonding electron on the N atom and the Li atom in the triplet state of $LiNH_2$. The Li–N–Li bonding of the $LiNH_2$ dimer is of the 3-center–2-electron type.

(4) From monomer **a1** to the singlet-state clusters, the change in N–H BDE values is small. By contrast, from monomer **a2** to the triplet clusters, the change in N–H BDE values is very large. The N–H bonds from singlet-state clusters are stable, while the N–H bonds for the triplet clusters dissociate easily when subjected to physical stimuli like heat or mechanical impact.

(5) Transformations from monomers (**a1**) to clusters are spontaneously exothermic processes. Monomer **a1** forms clusters (**b1**, **c1**, **d2** and **e1**) more easily at low temperature, and clusters with fewer numbers of rings tend to transfer to ones with more rings at low temperature.

(6) The calculated EA of LiNH is 0.27 eV. Ring-like $(LiNH_2)_{3,4}$ clusters possess higher VIE and E_g, but lower values of E_{HOMO}. E_g, E_{HOMO} and E_{av} decrease gradually, and then become constant. The calculated E_g value for **a1** is consistent with calculated $LiNH_2$ crystal results, but the calculated E_g values for **b1**, **c1**, **d1**–**d3** , **e1**–**e3**, **a2**, **b2** and **c2**–**c3** are slightly different from those calculated for $LiNH_2$ crystal. Ring-like $(LiNH_2)_{3,4}$ clusters are more stable than the others.

Acknowledgments We gratefully acknowledge support from the Key Laboratory for Attapulgite Science and Applied Technology of Jiangsu Province and the Natural Science Foundation of Jiangsu Province. S.Q.Z. thanks the Innovation Project for Postgraduates in Universities of Jiangsu Province (Grant No. CX09B093Z) for partial financial support.

References

1. Chen P, Xiong ZT, Luo JZ (2002) Nature 420:302–304
2. Leng HY, Ichikawa T, Hino S (2006) J Power Sources 156:166–170
3. Hinehliffe A (1977) Chem Phys Lett 45:88–91
4. Yoshino M, Kcaniya K, Takahashi Y (2005) J Alloys Compd 404–406:185–190
5. Burk P, Koppel I (1994) Int J Quantum Chem 51:313–318
6. Velikokhatnyi OI, Kumta PN (2007) Mater Sci Eng B 140:114–122
7. Tsumuraya T, Shishidou T, Oguchi T (2007) J Alloys Compd 446–447:323–327
8. Chen YH, Kang L, Zhang CR (2008) Acta Phys Sin 57:4174–4181
9. Chen YH, Kang L, Zhang CR (2008) Acta Chim Sin 66:2030–2036
10. Ge GX, Jing Q, Yang Z (2006) Acta Phys Sin 55:4548–4552
11. Jacobs H, Juza R (1972) Z Anorg Allg Chem 391:271–279
12. Miwa K, Ohba N, Towata S (2005) Phys Rev B 71:195109
13. Lee C, Yang W, Parr RG (1988) Phys Rev B 37:785–789
14. Becke AD (1992) J Chem Phys 97:9173–9177
15. Blanksby SJ, Ellison GB (2003) Acc Chem Res 36:255–263
16. Frisch MJ, Trucks GW, Schlegel HB et al (2003) Gaussian 03, Revision B.03. Gaussian, Pittsburgh
17. Douglas BG, Sheridan PM, Jihad IA (2001) J Am Chem Soc 123:5489–5494
18. Patrick B, Josik P, Georges T (1969) J Mol Struct 4:1–13
19. Linde G, Juza R (1974) Z Anorg Allg Chem 409:199–214
20. Philip AC, Paul AA, James WP (2007) J Alloys Compd 446–447:350–354
21. Bohger JPO, Eßman RR, Jacobs H (1995) J Mol Struct 348:325–328
22. Joseph WN, George CP (1965) Spectrochim Acta 21:877–882
23. Zhang CJ, Alavi A (2006) J Phys Chem B 110:7139–7143
24. Gupta M, Gupta RP (2007) J Alloys Compd 446–447:319–322
25. Scott AP, Radom L (1996) J Phys Chem 100:16502–16513
26. Orimo S, Nakamori Y, Eliseo JR (2007) Chem Rev 107:4111–4132
27. Celotta RJ, Bennett RA, Hall JL (1974) J Phys Chem 60:1740–1745